The Canadian Mineralogist
Vol. 33, pp. 77-84 (1995)

COMPLEX ZONING IN VESUVIANITE FROM THE CANIGOU MASSIF, PYRÉNÉES, FRANCE

ROGER L. GIBSON AND THOMAS WALLMACH*

Department of Geology, University of the Witwatersrand, Private Bag 3, P O WITS, 2050, Johannesburg, South Africa

DEON DE BRUIN

Geological Survey of South Africa, Private Bag X112, Pretoria 0001, South Africa

ABSTRACT

Vesuvianite grains in a calc-silicate layer from the Canigou massif (Pyrénées, France) display oscillatory concentric birefringence-zoning and a locally developed, discordant, nearly isotropic marginal zone. The boundaries between the zones correspond to sharp changes in the abundance of Ti, Al, Mg and Fe, although only Ti displays a consistent positive correlation with birefringence. Systematic variation in cation abundances also occurs within individual zones of equal birefringence, indicating that compositional zoning is, to some extent, independent of birefringence. Several schemes of cation substitution appear to have been operative in the vesuvianite, and different substitutions seem to have dominated at different times. The dominant substitutions in the higher-birefringence zones seem to be Ti + Mg $\rightleftharpoons$ 2Al and $Fe^{3+} \rightleftharpoons$ Al, whereas Mg $\rightleftharpoons Fe^{2+}$ may occur in addition to Ti + Mg $\rightleftharpoons$ 2Al in the lower-birefringence zones.

Keywords: calc-silicate, cation substitution, oscillatory birefringence zoning, Ti–Al–Mg–Fe zonation, vesuvianite, Canigou massif, Pyrénées, France.

SOMMAIRE

Les cristaux de vésuvianite dans un niveau à calc-silicates du massif du Canigou, dans les Pyrénées (France), font preuve de zonation concentrique de la biréfringence et, localement, du développement d'un liseré discordant et presque isotrope. Les contacts entre ces zones correspondent à des changements abrupts dans l'abondance de Ti, Al, Mg et Fe, quoique seul le Ti semble montrer une corrélation uniforme et positive avec la biréfringence. Une variation systématique avec l'abondance des cations se voit aussi à l'intérieur des zones biréfringentes, indiquant que la composition, jusqu'à un certain point, est indépendante de la biréfringence. Plusieurs schémas de substitution cationique semblent tour à tour avoir été importants dans la vésuvianite. Les schémas les plus importants dans les zones concentriques à biréfringence élevée semblent être Ti + Mg $\rightleftharpoons$ 2Al et $Fe^{3+} \rightleftharpoons$ Al, tandis que le couple Mg $\rightleftharpoons Fe^{2+}$ pourrait s'ajouter à Ti + Mg $\rightleftharpoons$ 2Al dans les zones concentriques à plus faible biréfringence.

(Traduit par la Rédaction)

Mots-clés: calc-silicate, substitution cationique, zonation oscillatoire en biréfringence, zonation en Ti–Al–Mg–Fe, vésuvianite, massif du Canigou, Pyrénées, France.

INTRODUCTION

Vesuvianite is a relatively common constituent of calc-silicate rocks in both regional and contact metamorphic environments. Studies of samples from a variety of localities have shown that it possesses a highly variable crystal chemistry (*e.g*., Hoisch 1985, Groat *et al.* 1992, 1993). Despite this evidence, however, only a few studies have dealt with compositional zoning within single crystals. Groat *et al.* (1993) have observed compositional variation in sector-zoned crystals and variations in mean atomic number corresponding to multiple concentric optical zones. Apart from this, however, only simple core-to-rim zoning has been reported: Arem (1973) attributed color zoning in vesuvianite crystals to variations in Cr and Mn, Kerrick *et al.* (1973) linked birefringence zoning to variable Ti content, and Hover Granath *et al.* (1983) mentioned core-to-rim variation of Ti and Fe^{3+}, but did not describe any accompanying variation in optical

---

* Present address: Department of Geology, University of Pretoria, Pretoria, 0002, South Africa.

characteristics. In this paper, we present the results of a detailed electron-microprobe investigation of vesuvianite from the Canigou massif (French Pyrénées) that exhibits unusual, complex birefringence-zoning. We discuss briefly the implications of these results for models of cation substitution for this mineral.

GEOLOGICAL SETTING

The Canigou massif is one of several massifs that together comprise the Axial Zone of the Pyrénées chain of mountains, situated between France and Spain. The massifs form part of a regional, low-pressure, greenschist–amphibolite-facies Hercynian metamorphic terrane of late Carboniferous age (Zwart 1986). In the Canigou massif, predominantly pelitic pre-Ordovician metasediments and intercalated Paleozoic orthogneisses have been metamorphosed up to the upper amphibolite facies (675 to 725°C, 4.0 to 4.5 kbar: Gibson & Bickle 1994). Numerous horizons of marble, some up to several tens of meters thick and containing subsidiary calc-silicate layers, occur within the metapelites (Guitard 1970).

Vesuvianite-bearing calc-silicate gneisses occur as layers within a folded horizon of white calcite marble approximately 1 km southeast of the Chalet des Cortalets, near the summit of the Canigou massif. Thermobarometry from adjacent garnet-bearing pelitic schists (Gibson 1989) indicates that the gneisses experienced peak metamorphic conditions of at least 600°C, 3.5–4.0 kbar. Vesuvianite occurs in a variety of parageneses with calcite, quartz, grossular, diopside and epidote. In several samples, individual grains of vesuvianite exhibit core-to-rim compositional zoning and, in one instance, this is accompanied by color zoning. The most unusual occurrence, however, involves vesuvianite that exhibits complex oscillatory birefringence-zoning (Fig. 1). The host rock for this vesuvianite is a mineralogically banded calc-silicate layer. The margin of the layer in contact with the surrounding marble comprises fine-grained polygonal quartz (90%), calcite (5%) and diopside (<5%). This is followed by a band comprising approximately equal amounts of grossular and calcite, with accessory quartz and poikiloblastic vesuvianite. The calcite occurs as fine-grained symplectitic intergrowths with the garnet, as coarse-grained aggregates in massive garnet, and within fractures in the garnet. Coarse calcite also occurs surrounding a sheaf-like aggregate of radiating grains of vesuvianite that are partially enclosed in massive garnet (Fig. 1a). The vesuvianite grains are idioblastic to subidioblastic and are up to 4 mm long. Some are slightly bent, and all are fractured. The third band comprises coarse-grained feldspar (35%) + diopside (25%) + grossular (25%) + vesuvianite (10%), with late clinozoisite (5%). The feldspar is predominantly K-feldspar, but plagioclase also is present. Optically continuous remnants of diopside in grossular and vesuvianite show a strong preferred elongation parallel to the banding. Based on textural relations, diopside is inferred to be the oldest phase, together with the fine-grained calcite and quartz. Vesuvianite and garnet enclose diopside, suggesting later growth, but both are partially replaced in turn by coarse-grained calcite, K-feldspar or clinozoisite. The sample is cut by fractures filled with calcite. Clinozoisite adjacent to the fractures replaces vesuvianite, and feldspar is commonly saussuritized.

VESUVIANITE

The idioblastic grains of vesuvianite in the sheaf-like aggregate differ from the stubbier, more irregular grains in the feldspar–diopside band in that they display concentric oscillatory birefringence-zoning (Fig. 1), whereas the stubby grains are optically homogeneous. Both types are uniaxial negative and may contain inclusions, typically of fine-grained vermicular calcite, quartz and occasional diopside. Some of the stubby grains are poikiloblastic, but the zoned grains contain relatively few inclusions, and these are generally concentrated in the core.

The vesuvianite in the sheaf-like aggregate displays cuspate to lobate margins against coarse-grained calcite (Fig. 1b), suggesting replacement of the vesuvianite by calcite. Unstrained calcite also occurs in fractures in the vesuvianite. The relationship between the vesuvianite and grossular is less clear, with idioblastic vesuvianite occasionally totally enclosed in garnet, but displaying straight faces suggestive of textural equilibrium (top, Fig. 1a). In other places, garnet appears to be partially or totally enclosed in vesuvianite. Like the vesuvianite, the grossular contains calcite-filled fractures and has been partially replaced by calcite.

The elongate grains of vesuvianite display up to nine dark (low-birefringence) zones alternating with lighter zones. Individual zones may be less than 10 μm in width. Under high magnification, the boundaries of the zones seem diffuse. Although the zoning is generally concentric, with the zone boundaries being straight and parallel to crystal faces, detailed examination of the grains shows a more complex picture, with individual zones varying in width, bifurcating and even dying out in places (Fig. 1b). Some zones are truncated by grain boundaries against calcite, garnet and even other grains of vesuvianite. In the case of vesuvianite–calcite boundaries, this truncation is clearly related to replacement of the vesuvianite by calcite. Where the truncation occurs at vesuvianite–garnet and vesuvianite–vesuvianite boundaries, however, the most likely explanation is that it is caused by interference between adjacent crystals during growth. On the left side of the diamond-shaped grain in Figure 1b, a dark, nearly isotropic, zone truncates the concentric zones. A similar zone is also found in the adjacent

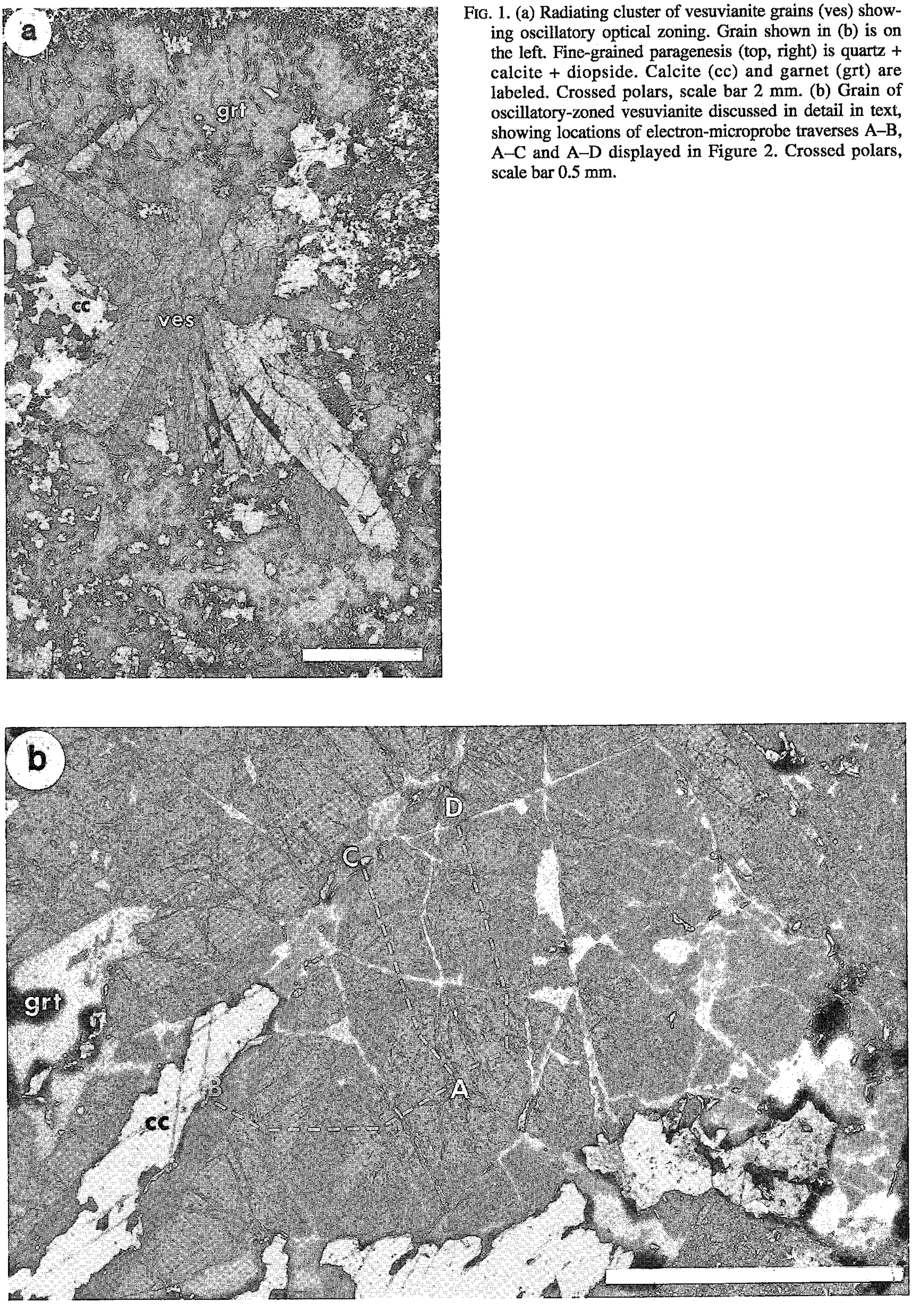

FIG. 1. (a) Radiating cluster of vesuvianite grains (ves) showing oscillatory optical zoning. Grain shown in (b) is on the left. Fine-grained paragenesis (top, right) is quartz + calcite + diopside. Calcite (cc) and garnet (grt) are labeled. Crossed polars, scale bar 2 mm. (b) Grain of oscillatory-zoned vesuvianite discussed in detail in text, showing locations of electron-microprobe traverses A–B, A–C and A–D displayed in Figure 2. Crossed polars, scale bar 0.5 mm.

grain of vesuvianite. Other grains also show a thin, discontinuous nearly isotropic marginal zone with a sharp boundary truncating the concentric birefringence-zones along parts of their boundaries with garnet and calcite. The margin displaying this zone in Figure 1b also has been partly resorbed by calcite.

No evidence was found of color zoning in these grains, and back-scattered electron images show no discernable contrasts in density corresponding to the birefringence zones.

COMPOSITIONAL DATA

Compositions were determined using a JEOL 733 electron microprobe at the Geological Survey of South Africa in Pretoria. Analyses were made in wavelength-dispersion mode at an accelerating potential of 15 kV and a sample current of 20 nA. A beam 1–2 μm wide was used to determine the fine-scale compositional variation indicated by the optical zoning. Counting times were 10 seconds on peaks and 2 × 5 seconds on background positions. Concentrations of Si, Al, Na and Mg were determined with TAP, of Ti, Cr and Ca, with PET, and of Fe and Mn, with LiF crystals. The standards for Si, Ca and Mg (diopside, Natural Bridge: USNM 117733), Al and Fe (Kakanui pyrope: USNM 143968), Na (Kakanui hornblende: USNM 143965) and Cr (chromite: USNM 117075) were described by Jarosewich *et al.* (1980). We used synthetic rutile and natural rhodonite as Ti and Mn standards.

A total of 74 analyses was made in three core-to-rim traverses across the diamond-shaped grain shown in Figure 1b. Additional spot-analyses were made of the zones in other grains to establish the consistency of these data. The results for profile A–B are listed in Table 1, and the variation in cation content along the three traverses is shown in Figure 2. The data in Table 1 are recorded to two decimal places because of the low standard deviations on minor elements and low detection-limits. Oxide totals were reduced to a 50-cation unit formula, as originally proposed by Coda *et al.* (1970), Rucklidge *et al.* (1975) and Hoisch (1985).

RESULTS

Calcium content varies in a narrow range from 18.6 to 19.2 apfu (atoms per formula unit). Sodium content is low, up to 0.13 apfu, but it is usually less than 0.10 apfu (Table 1). This is consistent with the results obtained by Groat *et al.* (1992), who noted that Na content is less than 0.2 apfu in vesuvianite with a Ti content less than 0.75 apfu. If the Na and Ca cation totals are combined, the resultant mean is 18.96 (standard deviation 0.13), statistically identical to the ideal value of 19 X sites indicated by the 50-cation formula. No consistent pattern was established between Ca and Na content and the variation in birefringence in the grain.

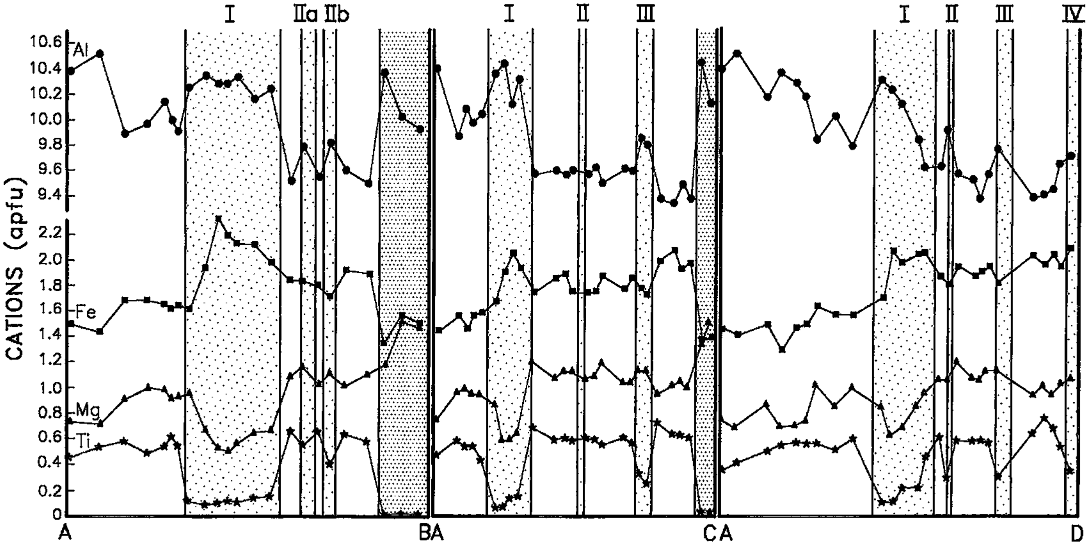

FIG. 2. Compositional profiles A–B, A–C and A–D across optically zoned vesuvianite shown in Figure 1b. Concentric low-birefringence zones are indicated with light stipple and labeled with Roman numerals. Nearly isotropic marginal zone shown in dark stipple.

TABLE 1. RESULTS OF CHEMICAL ANALYSES OF VESUVIANITE FROM TRAVERSE A–B (Fig. 1b)

#	23	22	21	20	19	18	17	16	15	14	13	12	11	10	9	8	7	6	5	4	3	2	1
Zone								I	I	I	I	I	I	I		IIa		IIb			Marginal zone		
SiO_2	36.70	36.40	36.45	36.52	35.62	36.46	36.24	36.39	36.30	36.11	36.30	36.32	36.57	36.53	36.43	36.62	36.74	36.41	35.93	36.47	36.63	36.54	36.78
TiO_2	1.27	1.45	1.57	1.33	1.44	1.62	1.48	0.32	0.22	0.27	0.29	0.26	0.35	0.40	1.76	1.48	1.77	1.09	1.67	1.57	-	0.01	-
Al_2O_3	17.84	18.13	17.05	17.07	17.36	17.09	17.04	17.52	17.64	17.59	17.58	17.69	17.39	17.67	16.40	16.94	16.50	16.91	16.35	16.32	17.92	17.39	17.26
Cr_2O_3	-	-	0.03	-	-	0.04	-	-	-	-	-	-	-	-	0.03	0.04	-	-	-	-	-	0.06	-
FeO	3.50	3.49	4.07	4.07	3.97	3.89	3.97	3.89	4.67	5.58	5.28	5.17	5.10	4.84	4.46	4.47	4.38	4.18	4.63	4.61	3.29	3.82	3.68
MnO	0.09	-	0.01	0.04	0.07	-	0.02	0.04	0.06	0.07	0.06	0.03	0.06	0.07	0.16	0.07	0.12	0.07	0.12	0.07	0.18	0.08	0.31
MgO	1.00	0.98	1.24	1.36	1.34	1.26	1.27	1.30	0.89	0.72	0.67	0.77	0.86	0.91	1.48	1.58	1.42	1.53	1.37	1.49	1.62	2.08	2.04
CaO	35.39	35.61	35.76	35.25	35.54	35.06	35.86	35.42	35.24	35.30	35.26	35.35	35.23	35.84	35.60	35.41	35.72	35.81	35.20	35.49	36.19	36.08	36.32
Na_2O	0.09	0.12	0.09	0.09	0.10	0.06	0.07	0.07	0.08	0.06	0.08	0.04	0.05	0.06	0.11	0.06	0.09	0.08	0.07	0.08	0.05	0.02	0.05
TOTAL	95.88	96.18	96.27	95.73	95.44	95.48	95.95	94.95	95.10	95.70	95.52	95.63	95.61	96.32	96.43	96.67	96.74	96.08	95.34	96.10	95.88	96.08	96.44
Si^{4+}	18.12	17.91	17.96	18.07	17.67	18.11	17.90	18.09	18.07	17.92	18.04	18.01	18.15	17.97	17.94	17.96	18.04	17.93	17.91	18.02	17.97	17.89	17.94
Ti^{4+}	0.47	0.54	0.58	0.49	0.54	0.61	0.55	0.12	0.08	0.10	0.11	0.10	0.13	0.15	0.65	0.55	0.65	0.40	0.63	0.58	-	0.01	-
Al^{3+}	10.38	10.51	9.90	9.96	10.15	10.00	9.92	10.26	10.35	10.29	10.29	10.34	10.17	10.25	9.52	9.79	9.55	9.82	9.60	9.50	10.36	10.03	9.92
Cr^{3+}	-	-	0.01	-	-	0.02	-	-	-	-	-	-	-	-	0.01	0.02	-	-	-	-	-	0.02	-
Fe^{2+}	1.45	1.44	1.68	1.68	1.65	1.62	1.64	1.62	1.94	2.32	2.19	2.14	2.12	1.99	1.84	1.83	1.80	1.72	1.93	1.90	1.35	1.56	1.50
Fe^{2+} *	0.83	0.95	0.58	0.64	0.80	0.62	0.56	0.88	1.29	1.61	1.48	1.48	1.29	1.24	0.36	0.62	0.35	0.54	0.53	0.40	0.71	0.59	0.42
Fe^{3+} *	0.62	0.49	1.10	1.04	0.85	1.00	1.08	0.74	0.65	0.71	0.71	0.66	0.83	0.75	1.48	1.21	1.45	1.18	1.40	1.50	0.64	0.97	1.08
Mn^{2+}	0.04	-	-	0.02	0.03	-	0.01	0.02	0.03	0.03	0.03	0.01	0.03	0.03	0.07	0.03	0.05	0.03	0.05	0.03	0.07	0.03	0.13
Mg^{2+}	0.74	0.72	0.91	1.00	0.99	0.93	0.94	0.96	0.66	0.53	0.50	0.57	0.64	0.67	1.09	1.16	1.04	1.12	1.02	1.10	1.18	1.52	1.48
Ca^{2+}	18.72	18.77	18.87	18.69	18.89	18.66	18.98	18.86	18.79	18.76	18.77	18.78	18.73	18.89	18.78	18.61	18.79	18.90	18.80	18.79	19.02	18.92	18.98
Na^{+}	0.09	0.11	0.09	0.09	0.10	0.06	0.07	0.07	0.08	0.06	0.08	0.04	0.05	0.06	0.11	0.06	0.09	0.08	0.07	0.08	0.05	0.02	0.05
ΣX^{+}	147.48	147.29	146.90	147.00	146.46	147.39	1.46.75	146.61	146.57	146.26	146.50	146.52	146.67	146.43	146.61	146.77	146.84	146.41	146.60	146.63	146.24	145.82	145.75

Analyses normalized on 50 total cations

* minimum Fe^{2+} and maximum Fe^{3+} calculated assuming 11 trivalent cations pfu

ΣX^{+} total cation charge assuming all Fe is Fe^{2+}

Si content varies slightly, from 17.7 to 18.3 apfu, with a mean of 17.99 (standard deviation 0.01). This finding, and the low skewness (–0.09), indicate that there is little or no Al-for-Si substitution at the *Z* sites.

The combined total for the remaining cations (Al^{3+}, Mg^{2+}, Fe^{2+}, Fe^{3+}, Ti^{4+}, Mn^{2+}) has a mean value of 13.09 (standard deviation 0.11), which is statistically identical to the ideal value of 13 *Y* sites. Al varies from 9.3 to 10.5 apfu, Mg from 0.5 to 1.5 apfu, and Fe from 1.3 to 2.3 apfu. Ti ranges from zero, in the nearly isotropic marginal zone, to 0.73 apfu. Mn content is negligible (0 to 0.04 apfu), but in analysis 1 (Table 1), it reaches 0.13 apfu.

Wavelength-dispersion scans failed to detect the presence of significant F peaks above the background. The vesuvianite along profile A–B was also analyzed for Cl, which was found only in the nearly isotropic marginal zone (0.15–0.23 wt%) and adjacent to a fracture (0.42 wt%). Boron was not sought, but indirect evidence suggests that the vesuvianite is B-free. This includes the optically negative nature of the vesuvianite, a low Mg content and high Al content, and the saturation of the *Z* cation site by Si (Groat *et al.* 1992).

Patterns of zoning

The variation in abundances of the main *Y*-site cations (Al, Fe, Mg, Ti) in the three core-to-rim traverses across the vesuvianite grain (Fig. 2) shows two patterns: (a) cation abundances differ sharply between zones with different birefringence, and (b) an overall decrease in Al, and an increase in Fe, occur across the grain from core to rim in the high-birefringence zones.

Kerrick *et al.* (1973) noted a link between birefringence and Ti abundance in vesuvianite crystals from the Twin Lakes area, California, although they neglected to stipulate the exact nature of the relationship. More recently, Deer *et al.* (1992) suggested that an inverse relationship exists between birefringence and the OH^- content of the vesuvianite. The slightly lower total charge in the nearly isotropic marginal zones of the vesuvianite investigated here (Table 1) is consistent with the relationship proposed by Deer *et al.* (1992); however, our inability to measure directly the OH^- content and the valence state of Fe in the different zones precludes a definitive statement on this relationship.

The data in Figure 2 indicate that Ti is the only cation that shows a consistent relationship with birefringence in all zones. Although Mg and Fe show significant variation across zone boundaries, Mg abundance decreases in zone I relative to the adjacent high-birefringence zones, but increases in the marginal zone. Fe shows the reciprocal relationship, increasing in zone I and decreasing in the marginal zone. Al abundance can also be discounted as a cause of the variable birefringence, as Al values for the different zones are similar (compare Al values for zone I, the marginal zone and the high-birefringence core zone in Fig. 2). In contrast, Ti decreases progressively with decreasing birefringence. The cutoff between the high- and low-birefringence concentric zones appears to be approximately 0.40 to 0.45 apfu, whereas the nearly isotropic marginal zone contains little, if any, Ti.

Implications of zoning for cation substitutions

Models of cation substitution for vesuvianite have been proposed by several investigators. Hoisch (1985) and Groat *et al.* (1992) proposed that the main substitution involving Ti in vesuvianite is $Ti + Mg \rightleftharpoons 2Al$. Valley *et al.* (1985) suggested that in Ti-free vesuvianite, $Fe^{3+} \rightleftharpoons Al$ is important. Groat *et al.* (1992) pointed out that involvement of anions in the cation substitutions could lead to a significant role for substitutions such as $Ti + O^{2-} \rightleftharpoons Al + OH^-$ and $Mg + OH^- \rightleftharpoons Al + O^{2-}$. They suggested that the latter substitution may be particularly significant because their study of a wide range of vesuvianite compositions failed to show sufficient variation in Ti to account for the observed variation in Al *via* the Ti–Al substitutions.

The cation–cation correlation diagrams in Figure 3 provide an indication of the most likely substitutions responsible for the zoning profiles in Figure 2. It is clear from these diagrams that zones of different birefringence contain different correlations, indicating a link between the zoning in birefringence and various cation substitutions. The poor inverse correlation between Ti and Al in the high-birefringence zones (dots, Fig. 3a), indicates that significant substitution for Al must occur by a means other than $Ti + Mg \rightleftharpoons 2Al$. The most likely candidate is the homovalent substitution $Fe^{3+} \rightleftharpoons Al$, evidence for which may be provided by the good inverse correlation between Fe_{TOTAL} and Al in the high-birefringence zones (Fig. 3d). This Fe^{3+}–Al substitution also may be important in the nearly isotropic marginal zone, although cation correlations in this zone are inconclusive. In contrast, the good inverse correlation between Ti and Al in the low-birefringence concentric zones (squares, Fig. 3a) suggests that $Ti + Mg \rightleftharpoons 2Al$ substitution is strong here (see also Figs. 3b, c). The poor correlation observed between Fe_{TOTAL} and Al (Fig. 3d) in these zones discounts $Fe^{3+} \rightleftharpoons Al$. Correlation between Mg and Fe_{TOTAL} also is poor (Fig. 3e); however, if we assume that the vesuvianite is saturated in trivalent cations, such that $Al + Fe^{3+} = 11$ apfu (see Groat *et al.* 1992), then the possibility of homovalent Mg–Fe^{2+} substitution can be tested. The resultant plot (Fig. 3f) suggests that such a substitution is plausible in the low-birefringence concentric zones.

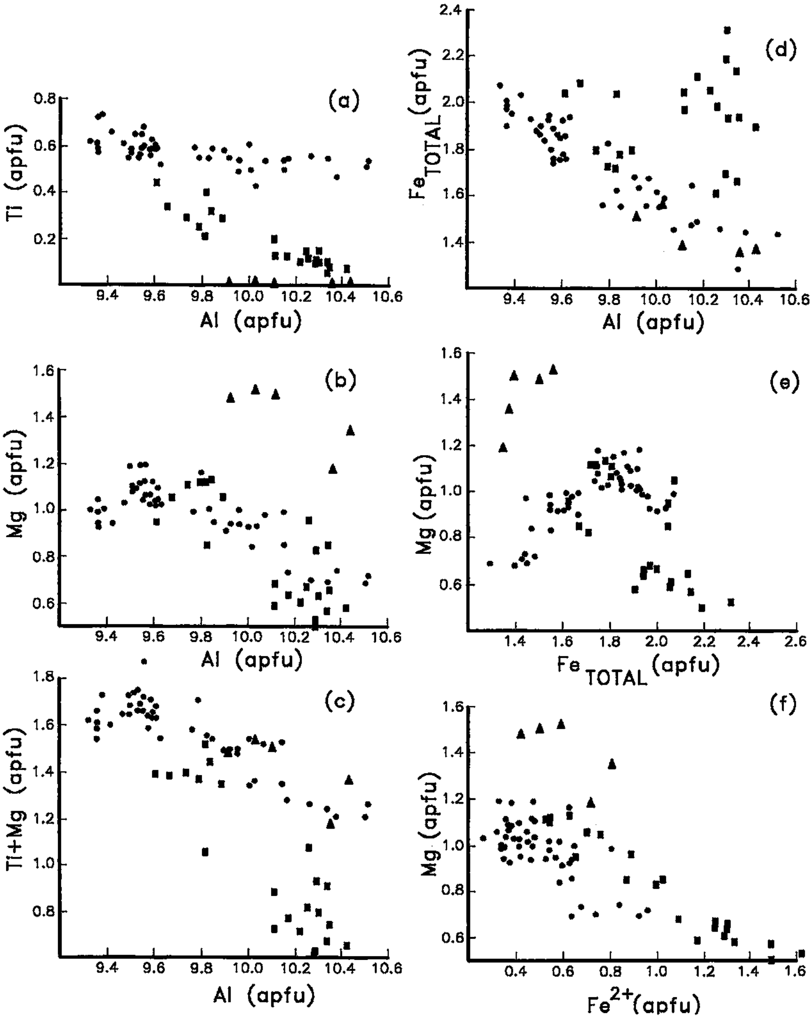

FIG. 3. Cation–cation correlation diagrams for data shown in Figure 2 (dots: high-birefringence concentric zones; squares: low-birefringence concentric zones; triangles: nearly isotropic marginal zone).

SUMMARY

(i) This study has recognized that vesuvianite may contain complex oscillatory zoning expressed in birefringence, which has important implications for understanding the crystal chemistry and mechanisms of cation substitution in this mineral.

(ii) The vesuvianite is zoned with respect to Ti, Al, Mg and Fe.

(iii) A positive correlation exists between the intensity of the birefringence in the grain and Ti abundance.

(iv) Cation zoning occurs within optically homogeneous birefringent zones and seems to reflect more than one substitution.

(v) Different substitutions appear to be operative in the low-birefringence zones ($Ti + Mg \rightleftharpoons 2Al$, $Mg \rightleftharpoons Fe^{2+}$) than in the high-birefringence zones ($Fe^{3+} \rightleftharpoons Al$, $Ti + Mg \rightleftharpoons 2Al$).

ACKNOWLEDGEMENTS

The sample discussed here was collected during RLG's Ph.D. studies at Cambridge University, England. Financial support was obtained from the University of the Witwatersrand Research Committee. DdB thanks the Director of the Geological Survey for permission to publish the data. R. Boer is thanked for his critical review of an early draft of this manuscript, and F.C. Hawthorne, R.F. Martin and two anonymous referees provided useful comments. L. Whitfield produced the diagrams, and M. Hudson, the photographs.

REFERENCES

AREM, J.E. (1973): Idocrase (vesuvianite) – a 250-year puzzle. *Mineral. Rec.* **4**, 164-174.

CODA, A., DELLA GIUSTA, A., ISETTI, G. & MAZZI, F. (1970): On the crystal structure of vesuvianite. *Atti Accad. Sci. Torino* **105**, 63-84.

DEER, W.A., HOWIE, R.A. & ZUSSMAN, J. (1992): *An Introduction to Rock-Forming Minerals* (second edition). J. Wiley & Sons, New York, N.Y.

GIBSON, R.L. (1989): *The Tectonic and Thermal Evolution of the Canigou Massif, Eastern Pyrenees.* Ph.D. thesis, Univ. Cambridge, Cambridge, England.

________ & BICKLE, M.J. (1994): Thermobarometric constraints on the conditions of metamorphism in the Canigou massif, Pyrenees: implications for Hercynian geothermal gradients. *J. Geol. Soc. Lond.* **151**, 987-997.

GROAT, L.A., HAWTHORNE, F.C. & ERCIT, T.S. (1992): The chemistry of vesuvianite. *Can. Mineral.* **30**, 19-48.

________, ________, ________ & PUTNIS, A. (1993): The symmetry of vesuvianite. *Can. Mineral.* **31**, 617-635.

GUITARD, G. (1970): Le métamorphisme hercynien mésozonal et les gneiss oeillés du massif du Canigou (Pyrénées Orientales). *Bur. Rech. Géol. Minières, Mém.* **63**.

HOISCH, T.D. (1985): The solid solution chemistry of vesuvianite. *Contrib. Mineral. Petrol.* **89**, 205-214.

HOVER GRANATH, V.C., PAPIKE, J.J. & LABOTKA, T.C. (1983): The Notch Peak contact metamorphic aureole, Utah: petrology of the Big Horse Limestone Member of the Orr Formation. *Geol. Soc. Am. Bull.* **94**, 889-906.

JAROSEWICH, E., NELEN, J.A. & NORBERG, J.A. (1980): Reference standards for electron microprobe analysis. *Geostand. Newsletter* **4**, 43-47.

KERRICK, D.M., CRAWFORD, K.E. & RANDAZZO, A.F. (1973): Metamorphism of calcareous rocks in three roof pendants in the Sierra Nevada, California. *J. Petrol.* **14**, 303-325.

RUCKLIDGE, J.C., KOEMAN, V., WHITLOW, S.H. & GABE, E.J. (1975): The crystal structures of three Canadian vesuvianites. *Can. Mineral.* **13**, 15-21.

VALLEY, J.W., PEACOR, D.R., BOWMAN, J.R., ESSENE, E.J. & ALLARD, M.J. (1985): Crystal chemistry of a Mg-vesuvianite and implications of phase equilibria in the system $CaO–MgO–Al_2O_3–SiO_2–H_2O–CO_2$. *J. Metamorph. Geol.* **3**, 137-153.

ZWART, H.J. (1986): The Variscan geology of the Pyrenees. *Tectonophys.* **129**, 9-27.

Received March 2, 1994, revised manuscript accepted September 12, 1994.